IAC-18,E2,1,2,x45262

Mapping Trajectories of an Asteroid that is Deflected by a Collision

Rodolfo B. Negri[a]*, Bruno Sarli[b], Antonio F. B. de A. Prado[a]

[a]*National Institute for Space Research, INPE, São José dos Campos, São Paulo, Brazil*, rodolfo.negri@inpe.br, antonio.prado@inpe.br
[b]*The Catholic University of America, Washington, District of Columbia, USA*, bruno.ren@gmail.com
* Corresponding Author

Abstract

An important task in the space community nowadays is to study what is the best form to avoid a collision of an asteroid with the Earth, what could possible save the Earth from huge material and lives losses. Several options have been considered, e.g. detonation of a nuclear artifact, gravity-tractor and kinect impactor. They can be separated into impulsive and non-impulsive alternatives. Among the impulsive approaches, the kinect impactor, changing the asteroid orbit by means of an impact between one or more spacecraft with it, is the most feasible for our current technological status. This papers aims to analyse the effects of Jupiter in this alternative by mapping the deflections obtained for several values of the impulse given to the asteroid by the kinect impact, as well as for the intercept time before the predicted closest approach with the Earth. In order to do so, we assume a Circular Restricted Three-Body Problem system composed by an asteroid, the Earth and the Sun; and a Bi-Circular Restricted Four-Body Problem system composed by an asteroid, the Earth, the Sun and Jupiter. The asteroid selected as a study case in this work has its orbital characteristics inspired in the asteroid 2017 PDC, from the hypothetical asteroid impact scenario presented at the 2017 IAA Planetary Defense Conference. The results obtained for the three-body problem are in accordance with previous studies in the literature, while the simulations considering Jupiter show that it can severely changes the outcome of such deflection strategy. The Jupiter addition to the dynamics causes a magnitude and phase shift in the predicted miss distance if compared to the three-body problem. In some cases this may increase the gravitational interaction between the Earth and the deflected asteroid and maybe culminates in large miss distances or impact scenarios that would not be predicted by the three-body problem. The present paper may be the first step for new studies of the Jupiter influence in an asteroid deflection.

Keywords: Kinect Impactor; Asteroid Deflection; Planetary Defense; Restricted Three-Body Problem; Bi-Circular Restricted Four-Body Problem.

1. Introduction

The recent incidents such as the Tunguska event in 1908 [1] and the Chelyabinsk meteor in 2013 [2] warn us that an asteroid collision with the Earth is a real risk. In the last decades, the possible threat of an asteroid impact with the Earth has gained much attention in the scientific community and many strategies have been proposed to deflect such an asteroid. They are mainly separated into two categories: impulsive and non-impulsive strategies. As an example of a non-impulsive alternative we can cite the gravity-tractor [3]. Among the impulsive approaches, the one considered in a more readiness technological status is the kinect impactor, in which one or more spacecraft impact the asteroid transferring momentum to it. In fact, in the next decade NASA should launch the DART spacecraft to test this deflection strategy [4].

Ahrens and Harris [5] derived one of the first analytical estimates of the necessary impulse to deflect an asteroid in a route of collision with the Earth. Park and Ross [6] formulated an optimization problem to find the minimal impulse to deflect the asteroid by using planar two-body approximations. Ross et al. [7] expanded this work by taking into account the gravitational effect of the Earth. A further generalization was made to consider the out of plane case [8]. Some of the main results of these and other works [9,10,11,12], that are considered in this paper, are: the impulse is more efficient if applied at the perihelion of the orbit of the asteroid; and the impulse is more efficient if applied in the direction of the velocity of the asteroid, for deflection times greater than roughly its orbital period.

The present paper aims to test the influence of Jupiter in an asteroid deflection. This is done by applying a complete three-body problem and then comparing it with a four-body problem. For this purpose, it is applied a CRTBP (Circular Restricted Three-Body Problem), which consists of the Earth, Sun and the Asteroid, and a BCRFBP (Bi-circular Restricted Four-Body Problem), composed by these three bodies with the addition of Jupiter. Additionaly, the analytical model presented in Carusi et al. [10] is applied to validate the results. The asteroid chosen to be deflected is inspired in the 2017 PDC, a hypothetical asteroid

impact scenario presented at the 2017 IAA Planetary Defense Conference.

2. Mathematical Formulation

It was chosen the CRTBP and the BCRFBP to analyse the effects of a third and a forth body, respectively, in the modification of the orbit of the asteroid due to the impulse received from a kinect impactor. The CRTBP is presented in Section 2.1 and the BCRFBP in Section 2.2. The Carusi et al. [10] analytical estimate used to validate the results is briefly presented in Section 2.3. In order to test the assumptions of the impulse applied to the asteroid, we apply the optimization method found in Park and Mazanek [8]. This is a three-dimensional optimization formulation that does not neglect the Earth and it is briefly stated in Section 2.4.

In the CRTBP and BCRFBP approaches a synodic reference frame is used and the equations of motion are written using the canonical system of units (the same is true for the analytical estimate and the optimization problem), which are: the unit of distance is the distance between M_1 and M_2, the gravitational constant is unitary, the angular speed of the synodic reference frame is unitary, the mass of M_2 is μ and the mass of M_1 is $1-\mu$, the unit of time is chosen such that the period of the synodic frame is 2π [13]. The synodic reference frame has its x axis connecting M_1 and M_2; its origin is the center of mass of M_1 and M_2; the y axis is orthogonal to the x axis lying on the orbital plane of M_1 and M_2 and the z axis completes the right handed reference frame.

2.1 Circular Restricted Three Body Problem (CRTBP)

To study the effect of the third body on the deflection of the asteroid it is chosen the CRTBP, where M_1 and M_2 are the Sun and the Earth, respectively, as shown in Fig. 1. The equations of motion are:

$$\ddot{x} - 2\,\dot{y} = x - (1-\mu)\frac{x+\mu}{r_1^3} - \mu\frac{x-1+\mu}{r_2^3}, \quad (2.1)$$

$$\ddot{y} + 2\,\dot{x} = y - (1-\mu)\frac{y}{r_1^3} - \mu\frac{y}{r_2^3}, \quad (2.2)$$

$$\ddot{z} = y - (1-\mu)\frac{z}{r_1^3} - \mu\frac{z}{r_2^3}, \quad (2.3)$$

where r_1 and r_2 are the distances between the Sun and the Earth to the asteroid, respectively.

2.2 Bi-Circular Restricted Four Body Problem (BCRFBP)

The BCRFBP is chosen to study the influence of Jupiter over the asteroid deflection. In this model, M_1 and M_2 are the Sun and Jupiter, respectively, as shown in Fig. 2. The Earth is assumed to be in a circular orbit around the center of mass of the Sun and Jupiter and on the same orbital plane. The equations of motion are:

$$\ddot{x} - 2\,\dot{y} - \frac{\mu_e}{R_e^2}\cos\psi = x - (1-\mu)\frac{x+\mu}{r_1^3} - \mu\frac{x-1+\mu}{r_2^3} - \frac{\mu_e}{r_3^3}(x - R_e\cos\psi), \quad (2.4)$$

$$\ddot{y} + 2\,\dot{x} + \frac{\mu_e}{R_e^2}\sin\psi = y - (1-\mu)\frac{y}{r_1^3} - \mu\frac{y}{r_2^3} - \frac{\mu_e}{r_3^3}(y - R_e\sin\psi), \quad (2.5)$$

$$\ddot{z} = -(1-\mu)\frac{z}{r_1^3} - \mu\frac{z}{r_2^3} - \frac{\mu_e}{r_3^3}z, \quad (2.6)$$

where r_1, r_2 and r_3 are the distances between the asteroid and the Sun, Jupiter and Earth, respectively. The angle ψ is the phase angle between Jupiter and the Earth, as shown in Fig. 2, μ_e is the mass of the Earth in canonical units (the actual mass of the Earth divided by the sum of the masses of Jupiter and the Sun) and R_e is the distance between the Earth and the center of the reference frame.

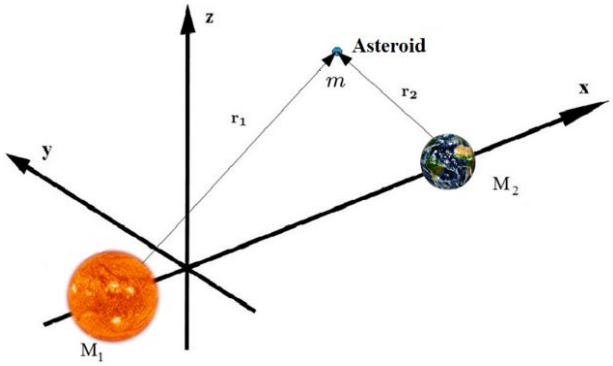

Fig. 1. Representation of the CRTBP.

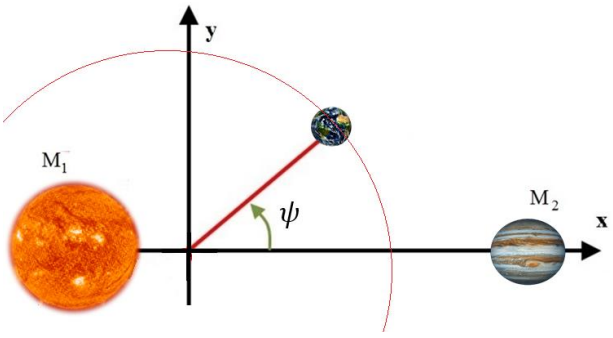

Fig. 2. Representation of the BCRFBP.

2.3 Analytical estimate

This analytical estimate takes into account the gravitational perturbation of the Earth, but differently of what is made in Carusi et al. [10], here we are interested in calculating the miss distance δ. Therefore, their analytical formulation can be simply restated to solve the following second order equation for the miss distance:

$$\delta^2 + \frac{2(1-\mu)}{U^2}\delta - b_i^2 = 0, \quad (2.7)$$

where the mass parameter μ is the same as the one of the CRTBP, and as a consequence all the other variables must be in accordance with the canonical units of the CRTBP as well, U is the heliocentric unperturbed encounter velocity and b_i is an impact parameter for the Earth, calculated here as:

$$b_i = \frac{(3\ t\ U\ sin\theta a\ V\ \Delta V)}{1 - 2\ a\ V\ \Delta V}, \quad (2.8)$$

where t is the time when the spacecraft intercepts the asteroid, θ is the angle between the asteroid's and Earth's velocities at the collision encounter, a is the semi-major axis of the asteroid, V is the velocity of the asteroid when the spacecraft impacts it and ΔV is the impulse applied to the asteroid due to the kinect impact. A more detailed description on how to calculate each of the parameters is presented in Carusi et al. [10].

2.4 Impulse Optimization

This method is formulated to calculate optimal impulses for deflecting the asteroid through nonlinear programming. It is applied a patched-conics approach, including the gravitational effect of the Earth.

The performance index is defined by the magnitude of the impulse applied to the asteroid as:

$$J = ||\Delta\vec{V}||, \quad (2.9)$$

while the constraints are stated as:

$$r_E - r_{SOI} = 0, \quad (2.10)$$
$$b - b_i =, \quad (2.11)$$
$$\dot{r}_E < 0, \quad (2.12)$$

in which r_E is the distance of the asteroid from the Earth, r_{SOI} is the radius of Earth's SOI, b is the approach distance of the asteroid and, finally, $\dot{r}_E$ is the time derivative of r_E. The impact parameter b_i is calculated different from the Eq. 2.8. For further explanations, please refer to Park and Mazanek [8].

3. Method

The semi-major axis (a = 2.2439 AU), inclination (i = 6.2970 degrees) and eccentricity (e = 0.6070) of the asteroid 2017 PDC is taken from the JPL's Horizon System. The inertial reference frame, represented in Fig. 3, is defined such that the center of the Earth lies in the x axis at the instant of the collision. The other three Keplerian elements of the asteroid (longitude of the ascending node, argument of periapsis and true anomaly) are found such that the orbit of the asteroid intersects exactly the position correspondent to the center of the Earth at the collision instant, in a two-body propagation. For the BCRFBP, it is assumed that the initial phase angle between Jupiter and the Earth is zero, meaning that Jupiter also lies in the x axis at the instant of the collision.

Once all of the orbital elements are obtained, the true anomaly is set a few degrees before the collision and the asteroid state at this point is obtained, which will be the initial state for our simulations. This procedure is necessary to avoid that the gravitational influence of the Earth severely changes the asteroid's orbital elements in the further backward integration of the equations of motion. The true anomaly offset is arbitrarily chosen in a way that the distance between the asteroid and the Earth is 2 to 3 times larger than the Earth's SOI. For the asteroid 2017 PDC a value of 5 degrees is good enough.

The equations of motion for each problem are integrated backward in time from 5 to 50 years. This range is considered for the time when the spacecraft intercepts the asteroid, when the $\Delta\vec{V}$ is applied. An 8-7th order Runge-Kutta integrator with Dormand and Prince formulae is chosen to integrate the equations of motion.

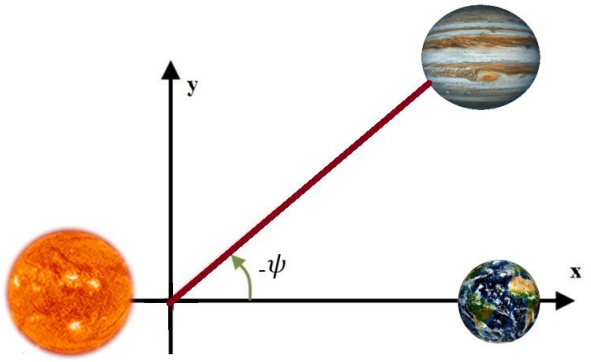

Fig. 3. The inertial reference frame at the collision instant.

As observed in other works [11,12], an impulse tangential to the velocity of the asteroid is the optimal solution when the intercept times are greater than about the orbital period of the asteroid. Therefore, we choose $\Delta\vec{V}$ to be tangential to the velocity of the asteroid, since our intercept time ranges from 5 to 50 years and the period of the asteroid is P = 3.35 years. The chosen $\Delta\vec{V}$ is applied to the asteroid state at the intercept instant and the equations of motion are then integrated forward in time, while keeping track of the relative distance between the asteroid and the Earth. The minimum relative distance between the asteroid and the Earth is admitted to be the miss distance δ.

4. Results and Discussion

This analysis indicates the divergence of the deflection obtained by a given $\Delta\vec{V}$, at an intercept time t,

between the three and four-body problems. The focus is to observe how sensible to the influence of Jupiter the deflection can be. This kind of analysis may be a precursor for further deeper studies in that line.

But, before investigating the divergence between the models, it is mandatory to prove that the assumptions of an optimal tangential impulse holds for the asteroid 2017 PDC in the time span considered here. This is done by applying the optimization problem described in Section 2.4.

Figures 4 and 5 show the optimal $\Delta\vec{V}$ obtained for different intercept times, decomposed into the tangential, perpendicular and normal components. Each component is defined as following: the tangential component is tangent to the asteroid's velocity; the perpendicular component is perpendicular to the first component and lies on the orbital plane of the asteroid and, lastly, the normal component is perpendicular to this orbital plane.

Figure 4 is obtained for a chosen miss distance of 1 Earth's radius. The tangential component is completely dominant for times greater than 5 years, as it is noticeable by the match between the green ($||\Delta\vec{V}||$) and the red (tangential component) curves. For most of the intercept times, the perpendicular component (blue line) is of the order of 0.1 mm/s and the normal component (black line) is less than 0.1 mm/s, not even being shown in the figure for most intercept times.

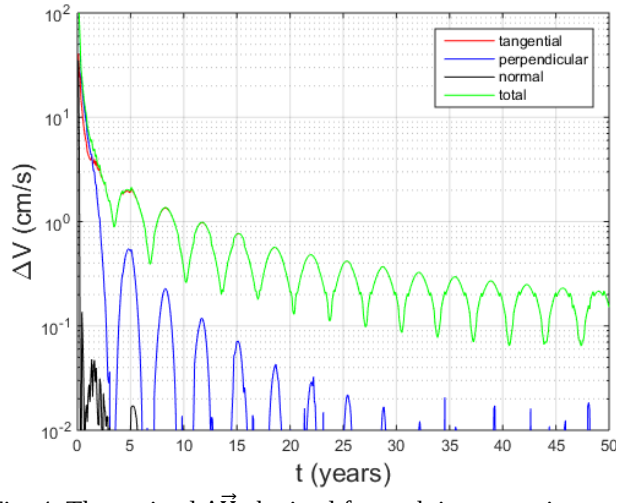

Fig. 4. The optimal $\Delta\vec{V}$ obtained for each intercept time, considering δ = 1 Earth's radius.

Figure 5 keeps the same framework, but now for a chosen miss distance of 100 Earth's radii. The tangential component stills dominant for times greater than five years, but with an increase of roughly two orders of magnitude.

Figures 6 to 9 show the miss distance for different values of the impulse. The perihelion points for the CRTBP and the BCRFBP are indicated by a red asterisk. As we will show, and as expected, the largest miss distances are achieved when the impulse is applied at the perihelion of the orbit of the asteroid. Yellow lines depict the results for the BCRFBP, while the orange lines represent the CRTBP and the blue lines the analytical estimate of the Section 2.3.

Figure 6 shows the results for an impulse of 1 cm/s. The analytical estimate shows a bounded linear behavior for the miss distance. This was expected because of the approximations in its formulation, which holds a linear relationship between the miss distance and the intercept time when the true anomaly is not considered. The CRTBP agrees quite well with the analytical estimate, which validates our formulation. The only significant divergence between both is found in the interval: 30 years < t < 45 years. This is probably caused by significant gravitational interactions between the asteroid and the Earth after the impulse is applied in this time interval. Such behavior was already noted by Carusi et al. [10]. In fact, they present a formulation to take into account these effects, which is disregarded in this paper. Finally, the BCRFBP diverges considerably from the other two. This is clear by the continuous phase shift between the BCRFBP and the other two models as the time grows. Moreover, the BCRFBP presents a maximum miss distance of 15.2 Earth's radii for the 50 year time span, while the analytical estimate and the CRTBP predicts a maximum miss distance of 18.5 Earth's radii. As already noted, all approaches predict the largest miss distances when the asteroid is at its perihelion.

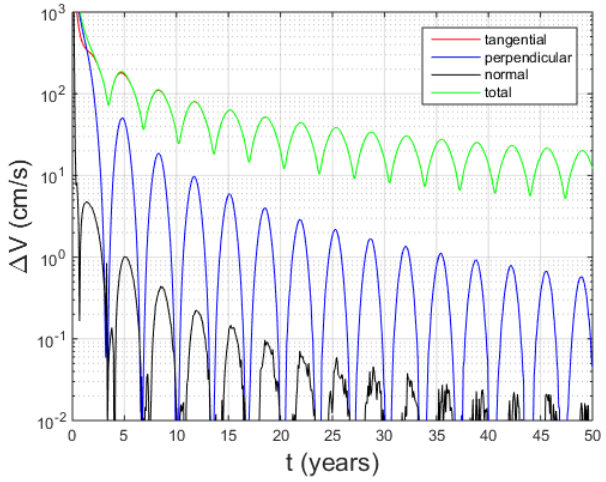

Fig. 5. The optimal $\Delta\vec{V}$ obtained for each intercept time, considering δ = 100 Earth's radii.

The same conclusions can be extended to Figs. 7 and 8. Figure 7 shows the results for an impulse of 5 cm/s. The maximum miss distance obtained for the BCRFBP is 76.6 Earth's radii while the CRTBP predicts that a maximum miss distance of 94.2 Earth's radii. This is

closely 5 times larger than the values predicted for an impulse of 1 cm/s, indicating a linear relationship between the impulse and the miss distance, what is expected for low impulses [5, 8]. For an impulse of 10 cm/s, shown in Fig. 8, the maximum miss distance under the BCRFBP is 154.6 Earth's radii and the CRTBP obtains a maximum miss distance of 189.4 Earth's radii. These values are closely 10 times larger than the ones obtained for an impulse of 1 cm/s.

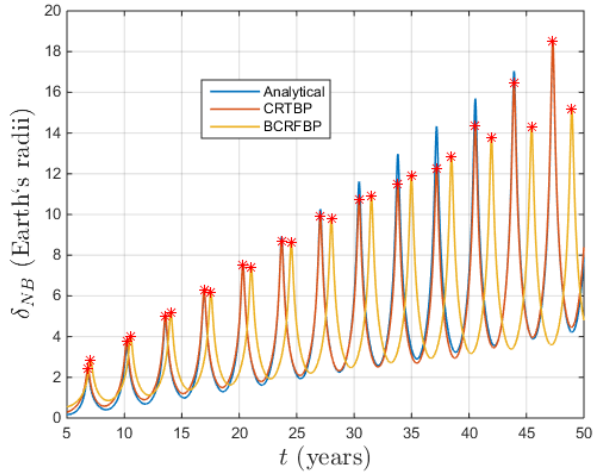

Fig. 6. The miss distance δ obtained for each of the models, using $||\Delta\vec{V}|| = 1\ cm/s$.

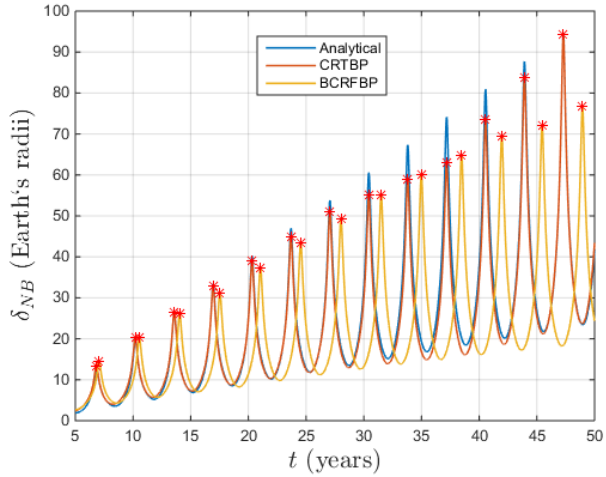

Fig. 7. The miss distance δ obtained for each of the models, using $||\Delta\vec{V}|| = 5\ cm/s$.

As noted in Fig. 5, a miss distance of 100 Earth's radii, which is very large (roughly 1.5 times the Earth-Moon distance), is obtained for greater intercept times with an impulse as low as ≈10 cm/s. Therefore, a value larger than this, in these conditions, would be unnecessary, if not infeasible from a technological and physical perspective related to the momentum transfer. However, for scientific purposes, extrapolating these considerations, and applying an impulse of 1 m/s, the Fig. 9 is obtained. The overall behavior is the same noted in the other figures. The maximum miss distance value is of 1721.9 for the BCRFBP and 1957.2 in the CRTBP, which is respectively 105.8 and 113.3 times larger than the values found for an impulse of 1 cm/s. This shows that the linear relationship between the miss distance and the impulse still roughly kept for impulses that could produce considerably large miss distances, at least for a long intercept time.

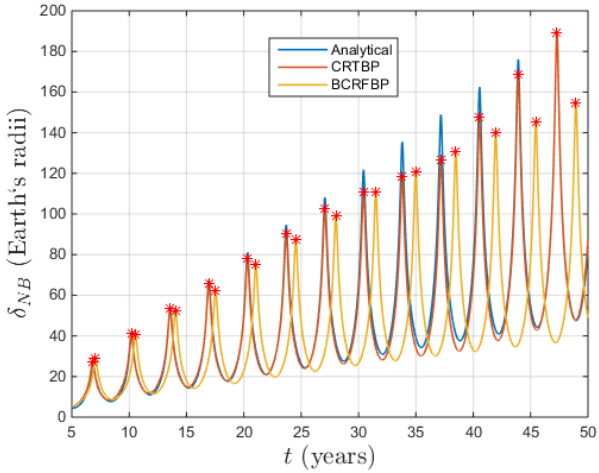

Fig. 8. The miss distance δ obtained for each of the models, using $||\Delta\vec{V}|| = 10$ cm/s.

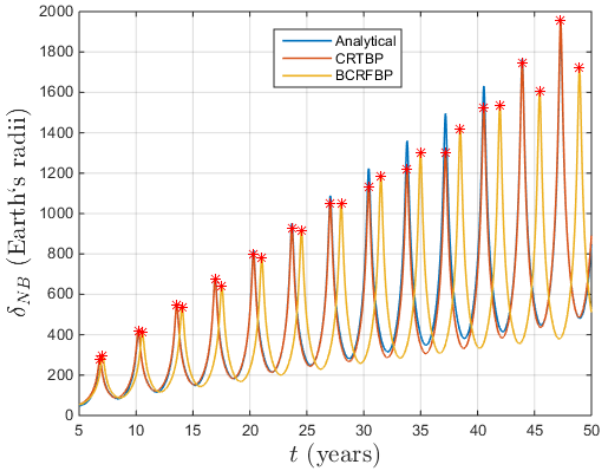

Fig. 9. The miss distance δ obtained for each of the models, using $||\Delta\vec{V}|| = 1\ m/s$.

The initial phase angle ψ is not a controllable variable. Of course, the Jupiter initial position cannot be chosen. However, by choosing different initial phase angles, the relevance of the Jupiter influence might become more obvious. For this reason, we now choose to apply an impulse of 1 cm/s for different Jupiter initial positions. The values chosen for the initial phase angle ψ are 90°, 180° and 270°, besides the already

applied value of 0º. Figures 10 to 13 show the results for an intercept time span of 15 to 50 years. The blue lines represent the CRTBP, while the orange lines are representing the BCRFBP. A red line is plotted to mark the Earth's radius.

Figure 10 shows the results for a phase angle of 0º. The results are the same obtained in Fig. 6, the only reason to plot it again is to keep the pattern with the later figures, what facilitates a comparison.

Figure 11 represents the results obtained for $\psi = 90º$, which means that Jupiter lies exactly on the inertial y axis at the collision instant between the asteroid and the Earth. As one can note, the phase shift between the miss distance curves of the BCRFBP and the CRTBP is largely reduced. Another interesting fact is that the BCRFBP predicts a maximum miss distance of roughly 18 Earth's radii when the initial phase angle is set to 90º, which is 3 Earth's radii larger than the one obtained for an angle value of 0º.

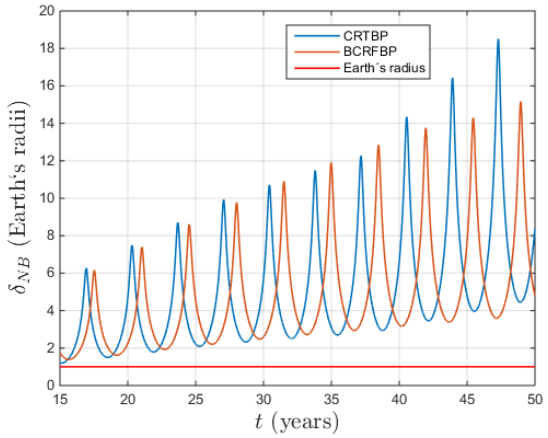

Fig. 10. The miss distance δ obtained for each of the models, using $||\Delta\vec{V}|| = 1\ cm/s$ and $\psi = 0º$.

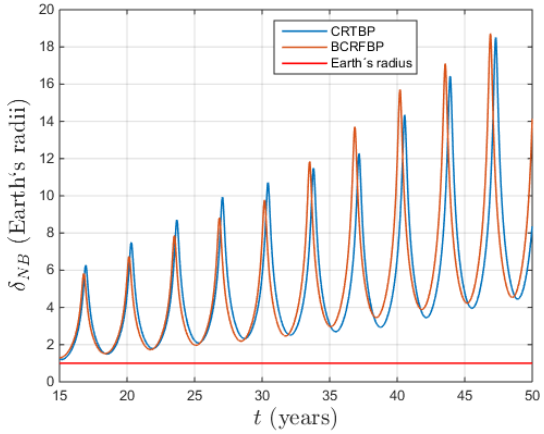

Fig. 11. The miss distance δ obtained for each of the models, using $||\Delta\vec{V}|| = 1\ cm/s$ and $\psi = 90º$.

If the initial phase angle is set to 180º, the results are very similar to the ones found for a value of 0º, as shown in Fig. 12. Nevertheless, some slight differences are noted. The miss distance curves are phase shifted backwards and a small divergence in the values are observed. The maximum miss distance for this case is close to 14 Earth's radii, while a roughly value of 15 Earth's radii is found in Fig. 10, as already shown.

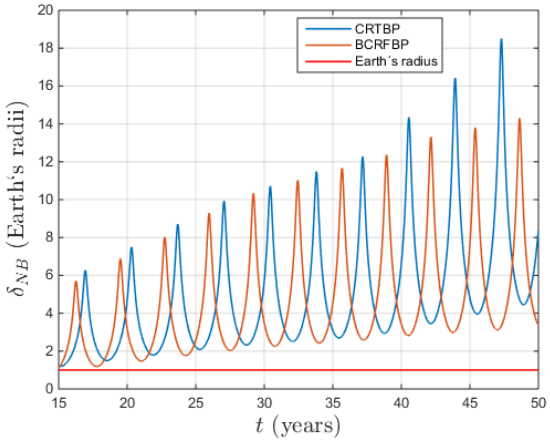

Fig. 12. The miss distance δ obtained for each of the models, using $||\Delta\vec{V}|| = 1\ cm/s$ and $\psi = 180º$.

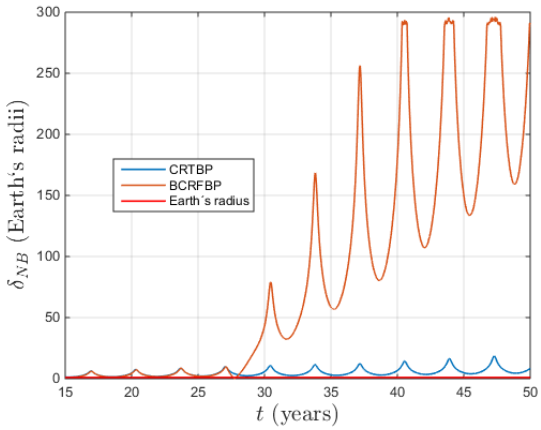

Fig. 13. The miss distance δ obtained for each of the models, using $||\Delta\vec{V}|| = 1\ cm/s$ and $\psi = 270º$.

Lastly, Fig. 13 shows the results when the initial phase angle is made equal 270º. The divergence between these results and the others are quite noticeable. In an intercept time of around 27 years, the miss distance value explodes in the BCRFBP, reaching up values as large as 300 Earth's radii. Zooming in Fig. 13 in lower miss distances we obtain the Fig. 14. It shows that the behavior for this case is quite similar to the one found in Fig. 11. However, when $t \approx 27$ years, the kinect impactor throw the asteroid in an orbit that causes an impact with the Earth. For larger intercept time values the miss distance explodes, indicating that

the Jupiter influence for this case causes a considerable gravitational interaction with the Earth if the impulse is applied.

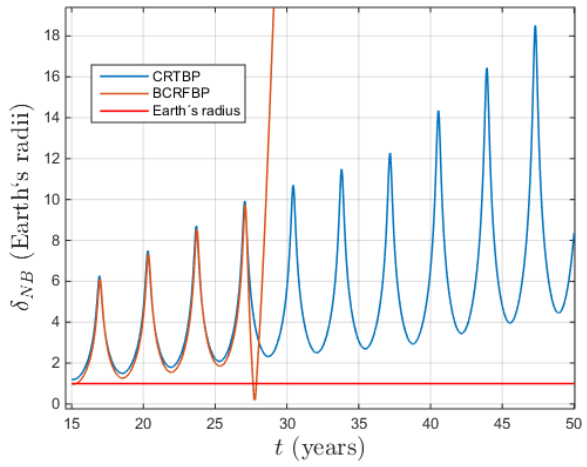

Fig. 14. Zooming in Fig.13.

5. Conclusions

The dynamics of an impulsive asteroid deflection considering the gravitational effects of the Earth and Jupiter was analyzed. They show that the effects of Jupiter might be considerable in some scenarios.

The linear relation between the miss distance and the impulse applied to the asteroid is held when considering the CRTBP. This is in accordance with previous studies in the literature and with the analytical estimate presented here. However, the simulations for the BCRFBP show that the Jupiter inclusion in the dynamics can substantially changes the relation. It can changes the magnitude of the obtained miss distance, the linear bounded relation between the time and the miss distance and also imply in a phase shift of the predicted miss distance.

Of course any predicted result obtained through a method similar to the one presented in Section 2.3 will be refined in a full N-body problem. Even so, if any analytical approximation or thumb rule considering Jupiter can be obtained, a first approach can predict a much more reliable result. And a behavior as harsh as the one obtained for an initial phase angle of 270º might be taken into account at a firsthand.

As far as the authors know, this is the first time that such a study is performed. Though Carusi et al. [10] made their analysis considering a full N-body problem, with Jupiter, Saturn, Mars, Moon and the Earth, no systematic attention was paid to compare the effects of each body. Therefore, this work may lay down the ground for further studies in the same lines.

Acknowledgements

The authors thank the grants # 406841/2016-0 and 301338/2016-7 from the National Council for Scientific and Technological Development (CNPq); and grants # 2017/20794-2, 2016/18613-7, 2015/19880-6, 2016/24561-0 and 2016/14665-2 from São Paulo Research Foundation (FAPESP).

References

[1] C. F. Chyba, Paul J. Thomas, and Kevin J. Zahnle, The 1908 Tunguska explosion: atmospheric disruption of a stony asteroid, Nature, 361.6407 (1993) 40.

[2] O. P. Popova, et al., Chelyabinsk airburst, damage assessment, meteorite recovery, and characterization, Science, v. 342, n. 6162, (2013) 1069-1073.

[3] E. T. Lu, S. G. Love, Gravitational tractor for towing asteroids, Nature, v. 438, n. 7065, (2005) 177.

[4] A. F. Cheng, J. Atchison, B. Kantsiper, A. S. Rivkin, A. Stickle, C. Reed, S. Ulamec, Asteroid impact and deflection assessment mission, Acta Astronautica, 115, (2015) 262-269.

[5] T. J. Ahrens, A. W. Harris, Deflection and fragmentation of near-Earth asteroids, Nature, 360(6403), (1992) 429.

[6] S.-Y. Park, I. M. Ross, Two-Body Optimization for Deflecting Earth-Crossing Asteroids, Journal of Guidance, Control, and Dynamics, Vol. 22, No. 3, (1999) 995–1002.

[7] I. M. Ross, S.-Y. Park, S. D. V. Porter, Gravitational Effects of Earth in Optimizing Δv for Deflecting Earth-Crossing Asteroids, Journal of Spacecraft and Rockets, Vol. 38, No. 5, Sept.–Oct. (2001) 759–764.

[8] S.-Y. Park, D. D. Mazanek, Mission functionality for deflecting Earth-crossing asteroids/comets, Journal of guidance, control, and dynamics 26.5 (2003) 734-742.

[9] D. Izzo, On the Deflection of Potentially Hazardous Objects, 15th AAS/AIAA Space Flight Mechanics Conference, Copper Mountain, CO, American Astronautical Society Paper (2005) 05-141.

[10] A. Carusi, G. B. Valsecchi, G. D'abramo, and A. Bottini, Deflecting NEOs in Route of Collision with the Earth, Icarus, Vol. 159, No. 12, (2002) 417–422.

[11] B. A. Conway, Near-Optimal Defection of Earth-Approaching Asteroids, Journal of Guidance, Control, and Dynamics, Vol. 24, No. 5, (2001) 1035–1037.

[12] M. Vasile, C. Colombo, Optimal impact strategies for asteroid deflection, Journal of guidance, control, and dynamics 31.4 (2008) 858-872.

[13] V. Szebehely, Theory of orbits: the restricted problem of three bodies, Academic Press, 1967.

[14] A. F. B. A. Prado, Searching for orbits with minimum fuel consumption for station-keeping

maneuvers: an application to lunisolar perturbations,
Mathematical Problems in Engineering, (2013).